Pole positions and residues from pion photoproduction using the Laurent+Pietarinen expansion method

Alfred Švarc*
Rudjer Bošković Institute, Bijenička cesta 54, P.O. Box 180, 10002 Zagreb, Croatia

Mirza Hadžimehmedović, Hedim Osmanović, and Jugoslav Stahov
University of Tuzla, Faculty of Science, Univerzitetska 4, 75000 Tuzla, Bosnia and Herzegovina

Lothar Tiator
Institut für Kernphysik, Universität Mainz, D-55099 Mainz, Germany

Ron L. Workman
Data Analysis Center at the Institute for Nuclear Studies, Department of Physics, The George Washington University, Washington, D.C. 20052

(Dated: April 8, 2014)

We have applied a new approach to determine the pole positions and residues from pion photoproduction multipoles. The method is based on a Laurent expansion of the partial wave T-matrices, with a Pietarinen series representing the regular part of energy-dependent and single-energy photoproduction solutions. The method has been applied to multipole fits generated by the MAID and GWU/SAID groups. We show that the number and properties of poles extracted from photoproduction data correspond very well to results from πN elastic data and values cited by Particle Data Group (PDG). The photoproduction residues provide new information for the electromagnetic current at the pole position, which are independent of background parameterizations, as opposed to the Breit-Wigner representation. Finally, we present the photo-decay amplitudes from the current MAID and SAID solutions at the pole, for all four-star nucleon resonances below $W = 2$ GeV.

PACS numbers: 11.55.-m, 11.55.Fv, 14.20.Gk, 25.40.Ny.

arXiv:1404.1544v1 [nucl-th] 6 Apr 2014

* alfred.svarc@irb.hr

I. INTRODUCTION

Revisions to the Review of Particle Properties, by the Particle Data Group (PDG) [1], and contributions to recent baryon spectroscopy workshops [2, 3] have emphasized the fact that poles, and not Breit-Wigner parameters, properly determine and quantify resonance properties linking scattering theory and QCD. However, the optimal method for extracting pole parameters, from single-channel T-matrices, remains an open question. Experimentalists are quite familiar with fits to data using Breit-Wigner functions (either with constant parameters and very general backgrounds, or with energy dependent masses and widths), but are less experienced when complex energy poles are desired. At present, poles are usually extracted from theoretical single or multi-channel models, which are first solved with free parameters fitted to the data. Only then is an array of standard pole extraction methods applied: analytic continuation of the model functions into the complex energy plane [4–8], speed plot [9], time delay [10], N/D method [11], regularization procedure [12], etc. However, this often requires continuing an obtained analytic solution, which implicitly contains both singular and regular (background) parts, into the complex energy plane. Consequently, the analytic form of the full solution, and its pole parameters, vary from model to model and the pole-background separation method requires an intimate knowledge of the underlying model.

In Ref. [13] we have presented a new approach to quantifying pole parameters of single-channel processes, based on a Laurent expansion of partial-wave T-matrices in the vicinity of the real axis. Instead of using the conventional power-series description of the non-singular part of the Laurent expansion, we have represented this using a convergent series of Pietarinen functions. As the analytic structure of the non-singular part is usually well understood (including physical cuts with branch points at inelastic thresholds, and unphysical cuts in the negative energy plane), we find that one Pietarinen series per cut represents the analytic structure fairly reliably. The number of terms in each Pietarinen series is determined by the quality of the fit. The method has been tested in two ways: on a toy model constructed from two known poles, various background terms, and two physical cuts, and on several sets of realistic πN elastic energy-dependent partial-wave amplitudes (GWU/SAID - [14, 15], and Dubna-Mainz-Taipei - [16, 17]). We have shown that the method is robust and stable, using up to three Pietarinen series, and is particularly convenient in fits to single-energy solutions, which are more directly tied to experiment. Apart from its ease of use, it provides a tool for the extraction and comparison of pole properties from different analyses. There have been several recent studies of model-dependence in single-energy photoproduction amplitude reconstruction [18] (both helicity and multipole), with extensions to other reactions as well [19]. The simplicity of the our expansion method enables us to self-consistently analyze and compare results from different approaches, as described below.

Here we have applied the new approach to determine pole positions and residues from single-pion photoproduction multipoles. The method has been applied to energy-dependent and single-energy multipole fits generated by the MAID and GWU/SAID groups for eight dominant multipoles. We show that the number and properties of poles extracted from photoproduction data correspond very well to results from πN elastic data and values cited by Particle Data Group (PDG) [1]. The photoproduction residues provide new information for the electromagnetic current at the pole position, which is independent of background parameterizations used in the Breit-Wigner approach.

With pole positions and residues, confidently determined for MAID and SAID ED solutions, we have further evaluated the photo-decay amplitudes at the pole positions and made a comparison with other very recent analyses.

Below, in Section II, we give an overview of the expansion method. In Section III, this method is applied to both energy-dependent and single-energy results from the MAID and SAID groups for eight dominant multipoles. At this point we also discuss our extended error analysis. In Section IV, we summarize and discuss our results for each partial wave. In section V, we present our photo-decay amplitudes and compare them to other recent extractions. Finally, in Section VI we summarize our results and conclude with prospects for further work.

II. FORMALISM

For the convenience of the reader, in this Section we outline the Laurent+Pietarinen (L+P) method, which is given a detailed description in Ref. [13].

A. Laurent (Mittag-Leffler) expansion

The starting point of our method is a generalization of the Laurent expansion, applied to multipoles, using the Mittag-Leffler theorem [13, 20], a theorem expressing a function in terms of its k first order poles and an entire

function:

$$T(W) = \sum_{i=1}^{k} \frac{a_{-1}^{(i)}}{W - W_i} + B^L(W); \quad a_{-1}^{(i)}, W_i, W \in \mathbb{C}. \tag{1}$$

Here, $a_{-1}^{(i)}$ and W_i are residua and pole positions for the i-th pole respectively, and $B^L(W)$ is a regular function in the whole complex plane. It is important to note that this expansion is not a representation of the unknown function $T(W)$ in the full complex energy plane, but is restricted to the part of the complex energy plane where the expansion converges, and is defined by the area of convergence of the Laurent expansion. If we choose poles as expansion points, the Laurent series converge on the open annulus around each pole, where the center of the annulus is the pole position. The outer radius of the annulus extends to the position of the next singularity (such as a nearby pole). Thus, our Laurent expansion converges on a sum of circles located at the poles, and this part of the complex energy plane in principle includes the real axis. Therefore, fitting the expansion (1) to the experimental data on the real axis, can in principle give the exact values of the scattering matrix poles.

The novelty of our approach is a particular choice for the non-pole contribution $B^L(W)$, based on an expansion method used by Pietarinen in the context of πN elastic scattering analysis. Before proceeding, we briefly review this method.

B. Pietarinen series

A specific type of conformal mapping technique has been proposed and introduced by Ciulli [21, 22] and Pietarinen [23], and used in the Karlsruhe-Helsinki partial wave analysis [24] as an efficient expansion of invariant amplitudes. It was later used by a number of authors for solving various problems in scattering and field theory [25], but not applied to the pole search prior to our recent study [13]. A more detailed discussion of the use of conformal mapping, and this method in particular, can be found in Refs.[13, 20].

If $F(W)$ is a general, unknown analytic function having a cut starting at $W = x_P$, then it can be represented in a power series of "Pietarinen functions" in the following way:

$$\begin{aligned} F(W) &= \sum_{n=0}^{N} c_n \, X(W)^n \,, \qquad W \in \mathbb{C} \,, \\ X(W) &= \frac{\alpha - \sqrt{x_P - W}}{\alpha + \sqrt{x_P - W}} \,, \quad c_n, x_P, \alpha \in \mathbb{R} \,, \end{aligned} \tag{2}$$

with α and c_n acting as tuning parameters and coefficients of the Pietarinen function, $X(W)$, respectively.

The essence of the approach is the fact that a set $(X(W)^n,\, n = 1,\, \infty)$ forms a complete set of functions defined on the unit circle in the complex energy plane having a branch cut starting at $W = x_P$. The analytic form of the function is, at the beginning, undefined. The final form of the analytic function $F(W)$ is obtained by introducing the rapidly convergent power series with real coefficients, and the degree of the expansion is automatically determined in fitting the input data. In the exercise of Ref.[23], as many as 50 terms were used; in the present case, covering a more narrow energy range, fewer terms are required.

C. Application of the Pietarinen series to scattering theory

The analytic structure of each partial wave is well known, with poles parameterizing resonant contributions, cuts in the physical region starting at thresholds of elastic and all possible inelastic channels, plus t-channel, u-channel and nucleon exchange contributions quantified with corresponding negative energy cuts. However, the explicit analytic form of each cut contribution remains to be determined. Instead of guessing the exact analytic form, we propose to use one Pietarinen series to represent each cut, with the number of terms determined by the quality of the fit to the input data. In principle, we have one Pietarinen series per cut, with known branch-points $x_P, x_Q ...$, and coefficients determined by the fit to a real physical process. In practice, we have too many cuts (especially in the negative energy range), thus we reduce their number by dividing them in two categories: all negative energy cuts are approximated with only one, effective negative energy cut represented by one (Pietarinen) series (we denote its branch point as x_P), while each physical cut is represented by a separate series with branch-points $(x_Q, x_R ...)$ determined by the physics of the process. In our present analysis, we fit all partial waves starting at the pion threshold. Therefore we fix our

second branch point, x_Q to the pion threshold at $W = 1077$ MeV. For the third branch point x_R we will compare results when a physical branch point is either fixed or fitted. Further branch points were found to be unnecessary in our present data analysis.

In summary, the set of equations which define the Laurent expansion + Pietarinen series method (L+P method) is:

$$
\begin{aligned}
T(W) &= \sum_{i=1}^{k} \frac{a_{-1}^{(i)}}{W - W_i} + B^L(W) \\
B^L(W) &= \sum_{n=0}^{M} c_n \, X(W)^n + \sum_{n=0}^{N} d_n \, Y(W)^n + \sum_{n=0}^{N} e_n \, Z(W)^n + \cdots \\
X(W) &= \frac{\alpha - \sqrt{x_P - W}}{\alpha + \sqrt{x_P - W}}; \quad Y(W) = \frac{\beta - \sqrt{x_Q - W}}{\beta + \sqrt{x_Q - W}}; \quad Z(W) = \frac{\gamma - \sqrt{x_R - W}}{\gamma + \sqrt{x_R - W}} + \cdots \\
& a_{-1}^{(i)}, W_i, W \in \mathbb{C} \\
& c_n, d_n, e_n \alpha, \beta, \gamma ... \in \mathbb{R} \text{ and } x_P, x_Q, x_R \in \mathbb{R} \text{ or } \mathbb{C} \\
& \text{and } \; k, M, N ... \in \mathbb{N}.
\end{aligned} \tag{3}
$$

As our input data are on the real axes, the fit is performed only on this dense subset of the complex energy plane. All Pietarinen parameters in set of equations (3) are determined by the fit.

We observe that the class of input functions which may be analyzed with this method is quite extensive. One may either fit partial-wave amplitudes obtained from theoretical models, or possibly experimental data directly. In either case, the T-matrix is represented by this set of equations (3), and minimization is usually carried out in terms of χ^2.

D. Real and complex branch points

While the fit strategy outlined in Eqs.(3) implies the use of purely real branch points, we know that there are, in principle, also complex branch points in the complex energy plane. This feature can be seen simply starting from three-body unitarity conditions [26]. However, real or complex branch points describe different physical situations. If the branch points x_P, x_Q.... are real numbers, this means that our background contributions are defined by stable initial and final state particles. All resonance contributions to the observed process are created by intermediate isobar resonances; all other initial and final state contributions are given by stable particles, and are described by Pietarinen expansions with real branch point coefficients. From experience, we know that this is not true: a three-body final state is always created, provided that the energy balance allows for it, and in three-body final states we typically do have a contribution from one stable particle (nucleon or pion), and many other combinations of two-body resonant sub-states, such as σ, ρ, Δ.... These resonant sub-states produce complex branch points.

As will be demonstrated below, we claim that the single-channel character of the L+P method prevents us from establishing, with certainty, which mechanism dominates. Specifically, with only single-channel information available, we have two alternatives: either we obtain a good fit with an extra resonance and stable initial and final state particles (real branch points), or we may obtain a good fit with one resonance fewer, and a complex branch point. Having only single-channel data, we are not able to distinguish between the two. This effect was already noted, in the context of the Jülich model, with a ρN complex branch point interfering and intermixing with the $N(1710)1/2^+$ resonance signature, as discussed in Ref. [27].

One advantage of the Pietarinen expansion method is its simple extension to complex branch points. We can check the above statements through applications of the L+P method to the photoproduction multipole $M_{1-}^{1/2}$, connected to the P_{11} partial wave from elastic pion-nucleon scattering.

III. APPLICATION OF THE L+P METHOD TO POLE EXTRACTION FROM PHOTOPRODUCTION MULTIPOLES

Fits to photoproduction data, particularly pion and kaon photoproduction, have been significantly advanced with the availability of new and precise measurements of polarization observables (both single- and double-polarization). This has revived the study of amplitude reconstruction from data with minimal theoretical input. However, significant discrepancies do still remain in comparisons of the major analyses. Results are generally reported either as energy-dependent (ED) fits, giving a functional representation of the amplitudes over some extended energy range, or as

single-energy (SE) solution, which analyze data in narrow bins of energy. In the SE case, a significant variation is possible, as a given bin does not generally contain a sufficient set of observables to uniquely determine an amplitude. Some constraints from the underlying ED fit are usually necessary to obtain a fit. Still, these SE fits do give a better representation of the data and can give hints of structure possibly missing in the global ED fit. It is therefore of interest to find a method of extracting resonance information from these, less smooth, sets of amplitudes. In the ED case, if one has the fit function, it is in principle possible to locate poles from a mapping of the amplitude in the complex energy plane.

In this paper we use the flexibility of the proposed L+P method (usable for both theoretical and experimental input), to extract pole parameters (pole positions and residues) for two well-known sets of ED and SE photoproduction amplitudes: the MAID[28] and GWU/SAID [14] results for single-pion photoproduction. Electric and magnetic multipole amplitudes are analyzed in the fits.

A. The fitting procedure

We use three Pietarinen functions (one with a branch-point in the unphysical region to represent all left-hand cuts, and two with branch-points in the physical region, to represent the dominant inelastic channels), combined with the minimal number of poles. In addition, we allow the possibility that one of the branch points becomes a complex number, accounting for all three-body final states in an effective manner. We generally start with 5 Pietarinen terms per decomposition, and the anticipated number of poles (one for most channels, two for $E_{0+}^{1/2}$). The discrepancy criteria are defined below in terms of reduced χ^2_{dp} for SE and its analog - discrepancy parameter D_{dp} for ED solutions. This quantity is minimized using MINUIT and the quality of the fit is also visually inspected by comparing the fitting function with fitted data. If the fit is unsatisfactory (discrepancy parameters are too high, or fit visually does not reproduce the fitted data), at first the number of Pietarinen terms is increased and, if this does not help, the number of poles is increased by one. The fit is repeated, and the quality of the fit is re-estimated. This procedure is continued until we have reached a satisfactory fit.

Pole positions, residues, and Pietarinen coefficients α, β, γ, c_i, d_i and e_i are our fitting parameters. However, in the strict spirit of the method, Pietarinen branch points x_P, x_Q and x_R should not be fitting parameters; we have declared that each known cut should be represented by its own Pietarinen series, fixed to known physical branch points. While this would be ideal, in practice the application is somewhat different. We can never include all physical cuts from the multi-channel process. Instead, we represent them by a smaller subset. Thus, in our model, Pietarinen branch points x_P, x_Q and x_R are not generally constants; we have explored the effect of allowing them to vary as fitting parameters. In the following, we shall demonstrate that when searched, the branch points in the physical region still naturally converge towards branch-points which belong to channels which dominate particular partial waves, but may not actually correspond to them exactly. The proximity of the fit results to exact physical branch points describes the "goodness of the fit", namely it tells us how well certain combinations of thresholds are indeed approximating a partial wave. And this, together with the choice of the degree of the Pietarinen polynomial, represents the model dependence of our method. We do not, of course, claim that our method is entirely model independent. However, the method chooses the simplest function with the given analytic properties which fits the data, and increases the complexity of the function only when the data require it.

B. Error analysis

In our principal paper [13] we have tested the validity of the model on a number of well known πN amplitudes, and concluded that the method is very robust and stable. However, in that paper we did not present an error analysis, deferring it to the forthcoming paper. We have fulfilled this promise in Ref. [29], and we repeat its essence for the convenience of the reader.

For energy-dependent solutions, we introduce the discrepancy or deviation parameter per data point D_{dp} (the substitute for χ^2 per data point, χ^2_{dp}, when analyzing experimental data) in the following way:

$$D_{dp} = \frac{1}{2\,N_E} \sum_{i=1}^{N_E} \left[\left(\frac{\mathrm{Re}T_i^{fit} - \mathrm{Re}T_i^{ED}}{Err_i^{\mathrm{Re}}} \right)^2 + \left(\frac{\mathrm{Im}T_i^{fit} - \mathrm{Im}T_i^{ED}}{Err_i^{\mathrm{Im}}} \right)^2 \right], \tag{4}$$

where N_E is the number of energies, and errors of energy-dependent solutions are introduced as:

$$Err_i^{\rm Re} = 0.05\ \frac{\sum_{k=1}^{N_E} |{\rm Re}T_k^{ED}|}{N_E} + 0.05\ |{\rm Re}T_i^{ED}|\,,$$
$$Err_i^{\rm Im} = 0.05\ \frac{\sum_{k=1}^{N_E} |{\rm Im}T_k^{ED}|}{N_E} + 0.05\ |{\rm Im}T_i^{ED}|\,.$$

When errors of the input amplitudes are not given, and one wants to make a minimization, errors have to be "defined". There are two simple ways to do it: either to assign a constant error to each data point, or introduce an energy-dependent error as a certain percentage of the given value. However, both definitions have drawbacks. For the first recipe only high-valued points are favored, while in the latter case low-valued points tend to be almost exactly reproduced. We find neither of these to be satisfactory, thus we follow prescriptions chosen by the GWU and Mainz groups, and use a sum of constant and energy dependent errors.

In the L+P method, we consider both statistical and systematic errors. Statistical errors are simply taken over from the MINUIT program, which is used for minimization. It is shown separately in all tables as the first term. Systematic errors are the errors of the method itself, and require a more detailed explanation. By construction it is clear that the method has its natural limitations. Our Laurent decomposition contains only two branch points in the physical region, and this is far from enough in a realistic case. Functions representing the multipole amplitudes, in principle containing more than two branch points, will in our model be approximated by a different analytic function containing only two. This approximation will be the main source of our errors. Therefore, we define the following procedure for quantifying systematic errors:

i) We completely release the first (unphysical) branch point x_P, as this represents a sum of many background contributions.

ii) We keep the first physical branch point x_Q fixed at $x_Q = 1077$ MeV (the πN threshold) because we know that this threshold branch point should always be present.

iii) The error analysis is done by varying the remaining physical branch point x_R in two ways:

a: We fix the third branch point x_R to the threshold of the dominant inelastic channel for the chosen partial wave (for instance η threshold for S-wave) if only one inelastic channel is important, or in case of several equally important inelastic processes we perform several fits with the x_R branch point fixed to each threshold in succession.

b: We release the third branch point x_R completely allowing MINUIT to find an effective branch point representing all inelastic channels. It is clear that if only one channel is dominant, the result of the fit will be very close to the dominant inelastic channel (see $S_{11}({}_pE_{0+})$ ($1486^{\eta N}$ vs. 1495^{free}) or otherwise in some effective location (see all other partial waves)

iv) We average results of the fit, and obtain a standard deviation

The list of all values for the branch point x_R is given in the Appendix.

The quality of our fits for the ED solutions is measured by the deviation D_{dp} defined in Eqs. (4) and (5).

For SE solutions we use the statistical errors and obtain the standard χ^2_{dp} definition:

$$\chi^2_{dp} = \frac{1}{2\,N_E}\ \sum_{i=1}^{N_E}\left[\left(\frac{{\rm Re}T_i^{fit} - {\rm Re}T_i^{SE}}{Err_i^{\rm Re}}\right)^2 + \left(\frac{{\rm Im}T_i^{fit} - {\rm Im}T_i^{SE}}{Err_i^{\rm Im}}\right)^2\right]\,, \tag{5}$$

where $Err_i^{\rm Re}$ and $Err_i^{\rm Im}$ are standard statistical errors of the SE solutions, real and imaginary parts respectively.

IV. RESULTS AND DISCUSSION ON PHOTOPRODUCTION MULTIPOLES

A. Real branch points

We have analyzed 24 partial wave amplitudes (electric and magnetic multipoles) from MAID and SAID solutions up to F waves. From this large number of results we have selected 8 important multipoles for detailed discussions:

${}_pE_{0+}^{1/2}, {}_pM_{1-}^{1/2}, E_{1+}^{3/2}, M_{1+}^{3/2}, {}_pE_{2-}^{1/2}, E_{2-}^{3/2}, {}_pE_{3-}^{1/2}, M_{3+}^{3/2}$. For the rest of the multipoles, we will present and discuss only the basic results.

In Tables I and II and in Figs. 1 - 4, we summarize results of all our fits for real branch points. We performed the analyses for ED and SE multipoles of the GWU/SAID CM12 solution [14] and the MAID MAID2007 solution [28].

Tables VIII and IX, given in the Appendix, summarize the results of the Pietarinen expansion parameters for real branch points. We show three branch points x_p, x_Q, x_R and the deviation D_{dp} in case of ED solutions and the χ^2_{dp} per data points in case of SE solutions. The latter ones should have a χ^2_{dp} close to 1. However, as the SE points are not always Gaussian distributed data points, the χ^2_{dp} values are generally in the range of $1-4$. For the ED solutions we have used an error definition, taking into account relative and absolute errors of the order of 5%. Therefore, for a good fit, the deviation D_{dp} is much smaller, in the range of $10^{-4} - 10^{-2}$. As already discussed in Sect. B, we have estimated the stability of our fits and the variation of the resonance parameters by applying 3 or 4 different assumptions for the effective $3rd$ branch point.

In Tables I and II, we present our results on the pole parameters of the nucleon resonances N^* and Δ that we found in our analysis. These are the pole positions W_p with $M_p = \mathrm{Re}\, W_p$ and $\Gamma_p = -2\,\mathrm{Im}\, W_p$ as well as (γ,π) residues in terms of magnitude and phase, $R_{\gamma,\pi} = |R_{\gamma,\pi}|\, e^{i\theta}$. Note, that the photoproduction residues, listed here, are not the residues of a (γ,π) T-matrix, but residues of the electromagnetic multipoles $E_{\ell\pm}$ and $M_{\ell\pm}$, which carry a dimension, e.g. mfm. Therefore, we use mfm GeV as a convenient dimension of $R_{\gamma,\pi}$.

In the following, we discuss our results in detail for each partial wave:

The S_{11} partial wave is the only case with two 4-star resonances. Both resonances are well determined from the ${}_pE_{0+}^{1/2}$ multipoles of the MAID and SAID analyses. Only for the second state, $N(1650)1/2^-$, we find a discrepancy in the strength, it appears two times as strong in the MAID analysis compared to SAID. A third resonance state, $N(1895)1/2^-$, is found, but only in the MAID ED solution. It shows up with a normalized strength of 2.5, a rather large value for a resonance only listed with 2-star. It will be an important candidate to watch for in forthcoming new SE analyses from complete experiment studies.

The P_{11} partial wave shows a consistency only for the existence of the Roper state $N(1440)1/2^+$. The second resonance state $N(1710)1/2^+$ (state with 3 PDG stars) is more problematic. It varies considerably in our analyses. The width differs by a factor 5 while the residue strength differs even more. In the MAID SE solution, see Fig. 3, a clear enhancement is seen in the imaginary part of the ${}_pM_{1-}^{1/2}$ multipole, near 1700 MeV. In the same region, however, the SAID SE solution in Fig. 4 appears rather smooth. This is another important case to be better determined with future double-polarization experiments. At this point, it is worth noting, that this state may also be compensated by different background parameterizations which both can similarly well describe the fitted data. One possible explanation for this problem can be given within the framework of L+P expansion method. Real branch points in the L+P method describe the situation when only two-body $\to$ two-body processes contribute, while the complex branch point is a mathematical implementation of the situation when the three-body final state, containing a two-body resonant sub-channel, is also important. When only real branch points are considered, this second $N(1710)1/2^+$ state is needed to explain the data. However, when a complex ρN branch point is used (indicating a resonance in the $\pi\pi$ sub-channel of a three-body final state), the second resonance in the πN channel is no longer needed. This will be further explored in the following subsection.

TABLE I. Pole positions in MeV and residues of four dominant isospin 1/2 multipoles as moduli in mfm · GeV and phases in degrees for real branch points. The results from L+P expansion are given for GWU/SAID and MAID energy-dependent (ED) and single-energy (SE) solutions. Resonances marked with a star indicate resonances which can be alternatively explained by the ρN complex branch point. Empty lines indicate that a resonance pole could not be found with a significant statistical weight.

Multipole	Source	Resonance	$\mathrm{Re}\,W_p$	$-2\mathrm{Im}\,W_p$	|residue|	θ
$S_{11}({}_pE_{0+})$	SAID ED	$N(1535)\ 1/2^-$	$1501 \pm 4 \pm 2$	$95 \pm 9 \pm 2$	$0.245 \pm 0.030 \pm 0.008$	$-(25 \pm 7 \pm 3)^\circ$
	MAID ED		$1516 \pm 1 \pm 2$	$94 \pm 3 \pm 2$	$0.234 \pm 0.009 \pm 0.004$	$-(2 \pm 3 \pm 7)^\circ$
	MAID SE		$1511 \pm 1 \pm 6$	$93 \pm 2 \pm 7$	$0.210 \pm 0.002 \pm 0.021$	$-(5 \pm 1 \pm 7)^\circ$
	SAID SE		$1501 \pm 1 \pm 2$	$112 \pm 2 \pm 7$	$0.312 \pm 0.003 \pm 0.022$	$-(18 \pm 1 \pm 3)^\circ$
	SAID ED	$N(1650)\ 1/2^-$	$1655 \pm 8 \pm 3$	$127 \pm 10 \pm 7$	$0.119 \pm 0.019 \pm 0.013$	$-(18 \pm 14 \pm 9)^\circ$
	MAID ED		$1678 \pm 2 \pm 2$	$135 \pm 3 \pm 2$	$0.289 \pm 0.010 \pm 0.009$	$+(12 \pm 3 \pm 4)^\circ$
	MAID SE		$1681 \pm 1 \pm 3$	$113 \pm 1 \pm 6$	$0.231 \pm 0.001 \pm 0.024$	$-(21 \pm 1 \pm 6)^\circ$
	SAID SE		$1650 \pm 1 \pm 1$	$117 \pm 2 \pm 14$	$0.153 \pm 0.002 \pm 0.026$	$-(8 \pm 5 \pm 5)^\circ$
	SAID ED	$N(1895)\ 1/2^-$	-	-	-	-
	MAID ED		$1913 \pm 4 \pm 8$	$258 \pm 10 \pm 37$	$0.327 \pm 0.015 \pm 0.2$	$-(68 \pm 4 \pm 10)^\circ$
	MAID SE		-	-	-	-
	SAID SE		-	-	-	-
$P_{11}({}_pM_{1-})$	SAID ED	$N(1440)\ 1/2^+$	$1360 \pm 4 \pm 1$	$183 \pm 10 \pm 9$	$0.290 \pm 0.015 \pm 0.039$	$-(61 \pm 4 \pm 1)^\circ$
	MAID ED		$1367 \pm 1 \pm 1$	$190 \pm 3 \pm 2$	$0.306 \pm 0.011 \pm 0.004$	$-(44 \pm 4 \pm 1)^\circ$
	MAID SE		$1379 \pm 2 \pm 4$	$183 \pm 3 \pm 5$	$0.394 \pm 0.003 \pm 0.005$	$-(36 \pm 1 \pm 5)^\circ$
	SAID SE		$1367 \pm 2 \pm 8$	$235 \pm 3 \pm 8$	$0.547 \pm 0.006 \pm 0.052$	$-(75 \pm 1 \pm 6)^\circ$
	SAID ED	$N(1710)^*\ 1/2^+$	$1789 \pm 9 \pm 4$	$550 \pm 25 \pm 3$	$0.609 \pm 0.031 \pm 0.014$	$+(98 \pm 3 \pm 4)^\circ$
	MAID ED		$1694 \pm 22 \pm 12$	$269 \pm 44 \pm 35$	$0.029 \pm 0.005 \pm 0.008$	$+(65 \pm 5 \pm 9)^\circ$
	MAID SE		$1678 \pm 5 \pm 3$	$99 \pm 14 \pm 23$	$0.062 \pm 0.006 \pm 0.012$	$-(16 \pm 4 \pm 2)^\circ$
	SAID SE		-	-	-	-
$D_{13}({}_pE_{2-})$	SAID ED	$N(1520)\ 3/2^-$	$1514 \pm 1 \pm 0$	$109 \pm 4 \pm 1$	$0.373 \pm 0.017 \pm 0.010$	$+(16 \pm 2 \pm 1)^\circ$
	MAID ED		$1509 \pm 1 \pm 0$	$106 \pm 1 \pm 1$	$0.375 \pm 0.003 \pm 0.001$	$+(11 \pm 1 \pm 1)^\circ$
	MAID SE		$1514 \pm 1 \pm 4$	$120 \pm 1 \pm 6$	$0.385 \pm 0.005 \pm 0.024$	$+(12 \pm 1 \pm 2)^\circ$
	SAID SE		$1514 \pm 1 \pm 1$	$111 \pm 1 \pm 0.5$	$0.382 \pm 0.004 \pm 0.003$	$+(14 \pm 1 \pm 3)^\circ$
	SAID ED	$N(1700)^*\ 3/2^-$	$1638 \pm 13 \pm 13$	$362 \pm 24 \pm 17$	$0.382 \pm 0.032 \pm 0.059$	$+(4 \pm 5 \pm 11)^\circ$
	MAID ED		-	-	-	-
	MAID SE		-	-	-	-
	SAID SE		$1654 \pm 5 \pm 15$	$257 \pm 10 \pm 47$	$0.187 \pm 0.007 \pm 0.080$	$-(1 \pm 3 \pm 7)^o$
$F_{15}({}_pE_{3-})$	SAID ED	$N(1680)\ 5/2^+$	$1674 \pm 2 \pm 0.5$	$113 \pm 4 \pm 0$	$0.157 \pm 0.008 \pm 0$	$-(5 \pm 3 \pm 0)^\circ$
	MAID ED		$1663 \pm 1 \pm 0$	$118 \pm 2 \pm 1$	$0.150 \pm 0.003 \pm 0.001$	$-(3 \pm 1 \pm 1)^\circ$
	MAID SE		$1669 \pm 1 \pm 1$	$113 \pm 1 \pm 1$	$0.145 \pm 0.005 \pm 0.002$	$+(2 \pm 1 \pm 1)^\circ$
	SAID SE		$1677 \pm 1 \pm 1$	$115 \pm 1 \pm 3$	$0.174 \pm 0.002 \pm 0.008$	$+(1 \pm 1 \pm 2)^\circ$
	SAID ED	$N(2000)^*\ 5/2^+$	-	-	-	-
	MAID ED		$1801 \pm 14 \pm 4$	$141 \pm 28 \pm 13$	$0.007 \pm 0.002 \pm 0.003$	$+(32 \pm 14 \pm 9)^\circ$
	MAID SE		-	-	-	-
	SAID SE		$1923 \pm 4 \pm 68$	$172 \pm 30 \pm 22$	$0.081 \pm 0.004 \pm 0.047$	$+(62 \pm 3 \pm 87)^\circ$

TABLE II. Pole positions in MeV and residues of four dominant isospin 3/2 multipoles as moduli in mfm · GeV and phases in degrees for real branch points. The results from L+P expansion are given for GWU/SAID and MAID energy-dependent (ED) and single-energy (SE) solutions. Empty lines indicate that a resonance pole could not be found with a significant statistical weight.

Multipole	Source	Resonance	$\mathrm{Re}\, W_p$	$-2\mathrm{Im}\, W_p$	|residue|	θ
$P_{33}(E_{1+})$	SAID ED	$\Delta(1232)\ 3/2^+$	$1211 \pm 0.5 \pm 1$	$101 \pm 1 \pm 0$	$0.183 \pm 0.005 \pm 0.001$	$-(154 \pm 1 \pm 1)^\circ$
	MAID ED		$1211 \pm 0.5 \pm 0.5$	$99 \pm 0.5 \pm 0.5$	$0.184 \pm 0.002 \pm 0.003$	$-(155 \pm 1 \pm 1)^\circ$
	MAID SE		$1215 \pm 0 \pm 4$	$87 \pm 0 \pm 1$	$0.154 \pm 0.001 \pm 0.010$	$-(155 \pm 0 \pm 8)^\circ$
	SAID SE		$1220 \pm 1 \pm 1$	$85 \pm 1 \pm 2$	$0.146 \pm 0.002 \pm 0.002$	$-(143 \pm 1 \pm 1)^\circ$
	SAID ED	$\Delta(1600)\ 3/2^+$	$1470 \pm 16 \pm 15$	$396 \pm 34 \pm 17$	$0.127 \pm 0.099 \pm 0.014$	$+(109 \pm 5 \pm 15)^\circ$
	MAID ED		$1550 \pm 7 \pm 4$	$347 \pm 12 \pm 29$	$0.087 \pm 0.005 \pm 0.019$	$+(127 \pm 5 \pm 4)^\circ$
	MAID SE		-	-	-	-
	SAID SE		-	-	-	-
$P_{33}(M_{1+})$	SAID ED	$\Delta(1232)\ 3/2^+$	$1211 \pm 0.5 \pm 0.5$	$101 \pm 1 \pm 1$	$2.974 \pm 0.013 \pm 0.028$	$-(26 \pm 1 \pm 1)^\circ$
	MAID ED		$1209 \pm 0.5 \pm 0.5$	$99 \pm 0.5 \pm 0.5$	$2.963 \pm 0.021 \pm 0.040$	$-(31 \pm 1 \pm 1)^\circ$
	MAID SE		$1210 \pm 0 \pm 1$	$100 \pm 0 \pm 1$	$3.010 \pm 0.003 \pm 0.020$	$-(30 \pm 0 \pm 1)^\circ$
	SAID SE		$1211 \pm 0 \pm 0.5$	$101 \pm 0 \pm 1$	$3.008 \pm 0.002 \pm 0.033$	$-(27 \pm 0 \pm 1)^\circ$
	SAID ED	$\Delta(1600)\ 3/2^+$	$1522 \pm 12 \pm 7$	$409 \pm 24 \pm 11$	$1.195 \pm 0.100 \pm 0.104$	$-(132 \pm 2 \pm 6)^\circ$
	MAID ED		$1498 \pm 10 \pm 22$	$326 \pm 20 \pm 20$	$0.499 \pm 0.005 \pm 109$	$-(149 \pm 1 \pm 20)^\circ$
	MAID SE		-	-	-	-
	SAID SE		$1512 \pm 3 \pm 14$	$408 \pm 5 \pm 39$	$1.173 \pm 0.016 \pm 0.205$	$-(144 \pm 1 \pm 9)^\circ$
$D_{33}(E_{2-})$	SAID ED	$\Delta(1700)\ 3/2^-$	$1650 \pm 4 \pm 0$	$255 \pm 8 \pm 3$	$0.672 \pm 0.026 \pm 0.022$	$-(177 \pm 2 \pm 1)^\circ$
	MAID ED		$1649 \pm 1 \pm 1$	$223 \pm 2 \pm 2$	$0.874 \pm 0.004 \pm 0.011$	$-(175 \pm 1 \pm 2)^\circ$
	MAID SE		$1671 \pm 0 \pm 10$	$376 \pm 1 \pm 6$	$1.792 \pm 0.001 \pm 0.169$	$-(160 \pm 1 \pm 8)^\circ$
	SAID SE		$1662 \pm 1 \pm 3$	$324 \pm 2 \pm 6$	$1.075 \pm 0.010 \pm 0.044$	$-(161 \pm 1 \pm 3)^\circ$
$F_{37}(M_{3+})$	SAID ED	$\Delta(1950)\ 7/2^+$	$1884 \pm 3 \pm 1$	$231 \pm 8 \pm 1$	$0.278 \pm 0.016 \pm 0.003$	$-(16 \pm 2 \pm 1)^\circ$
	MAID ED		$1898 \pm 1 \pm 1$	$271 \pm 3 \pm 1$	$0.339 \pm 0.009 \pm 0.003$	$-(11 \pm 1 \pm 1)^\circ$
	MAID SE		$1880 \pm 1 \pm 7$	$240 \pm 1 \pm 9$	$0.283 \pm 0.003 \pm 0.033$	$-(24 \pm 1 \pm 6)^\circ$
	SAID SE		$1882 \pm 1 \pm 1$	$236 \pm 2 \pm 2$	$0.283 \pm 0.003 \pm 0.004$	$-(17 \pm 1 \pm 1)^\circ$

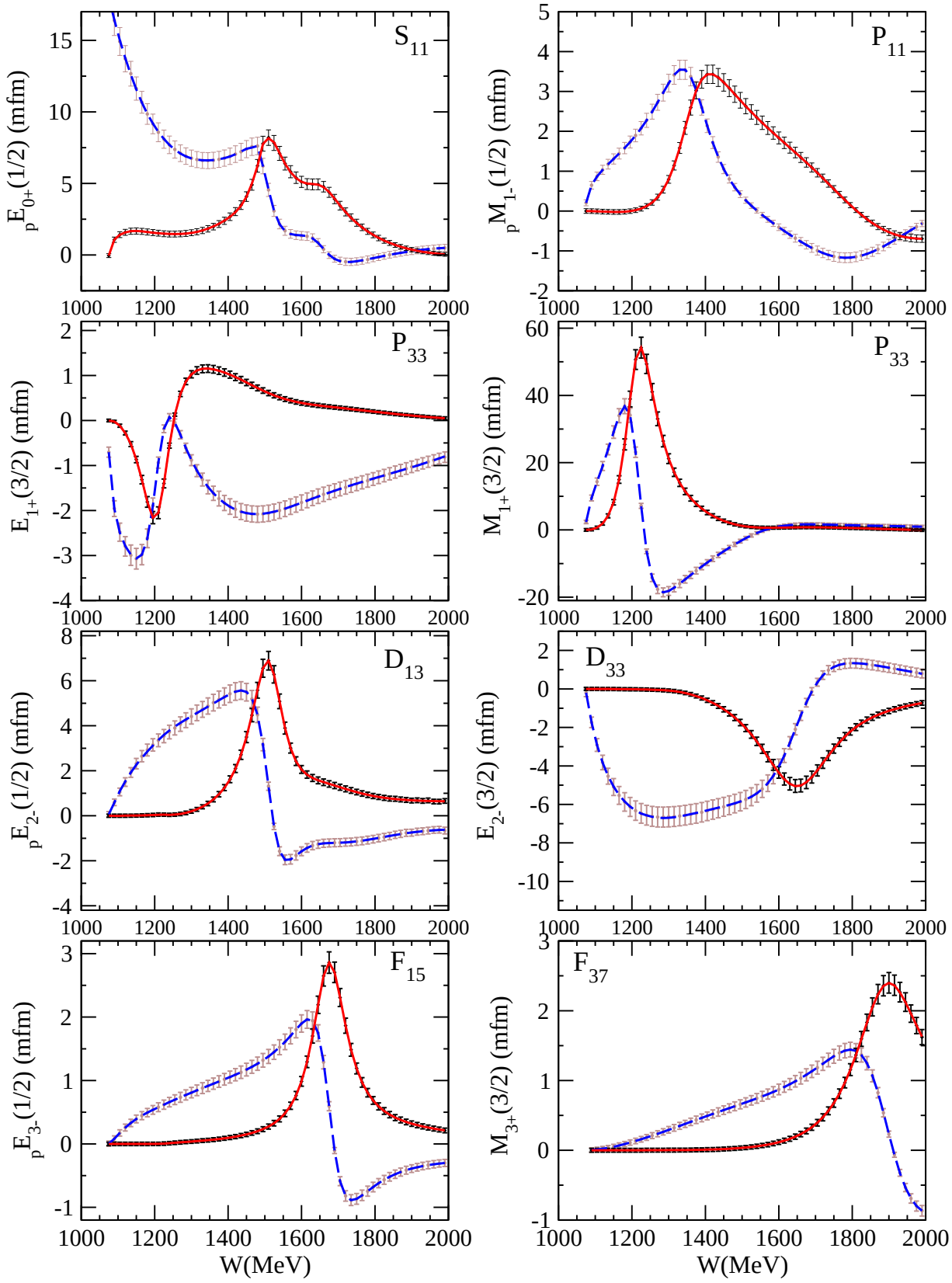

FIG. 1. L+P fit to GWU/SAID CM12 ED solutions. Dashed blue, and full red lines denote real and imaginary parts of multipoles respectively.

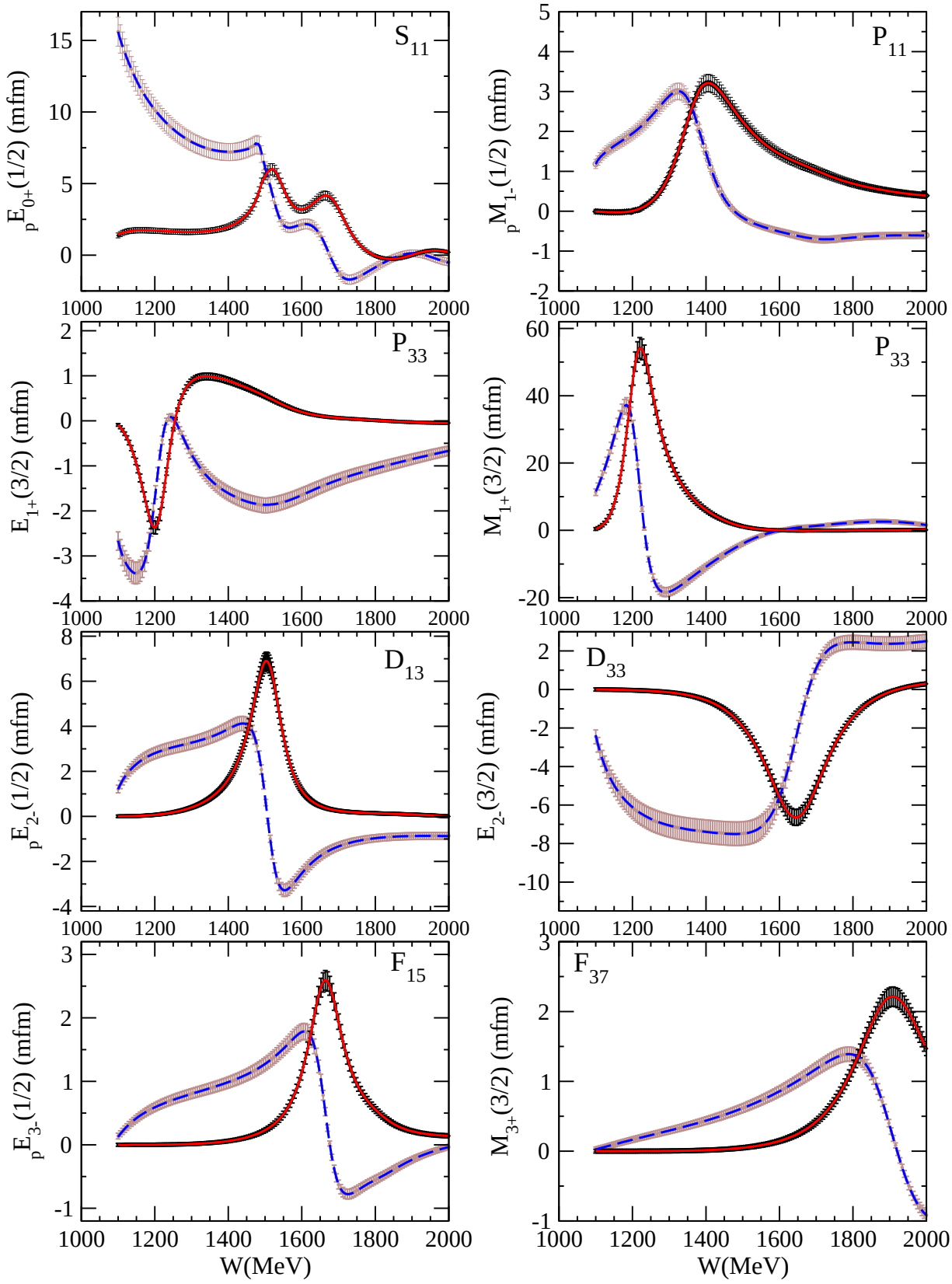

FIG. 2. L+P fit to MAID MAID2007 ED solutions. Dashed blue, and full red lines denote real and imaginary parts of multipoles respectively.

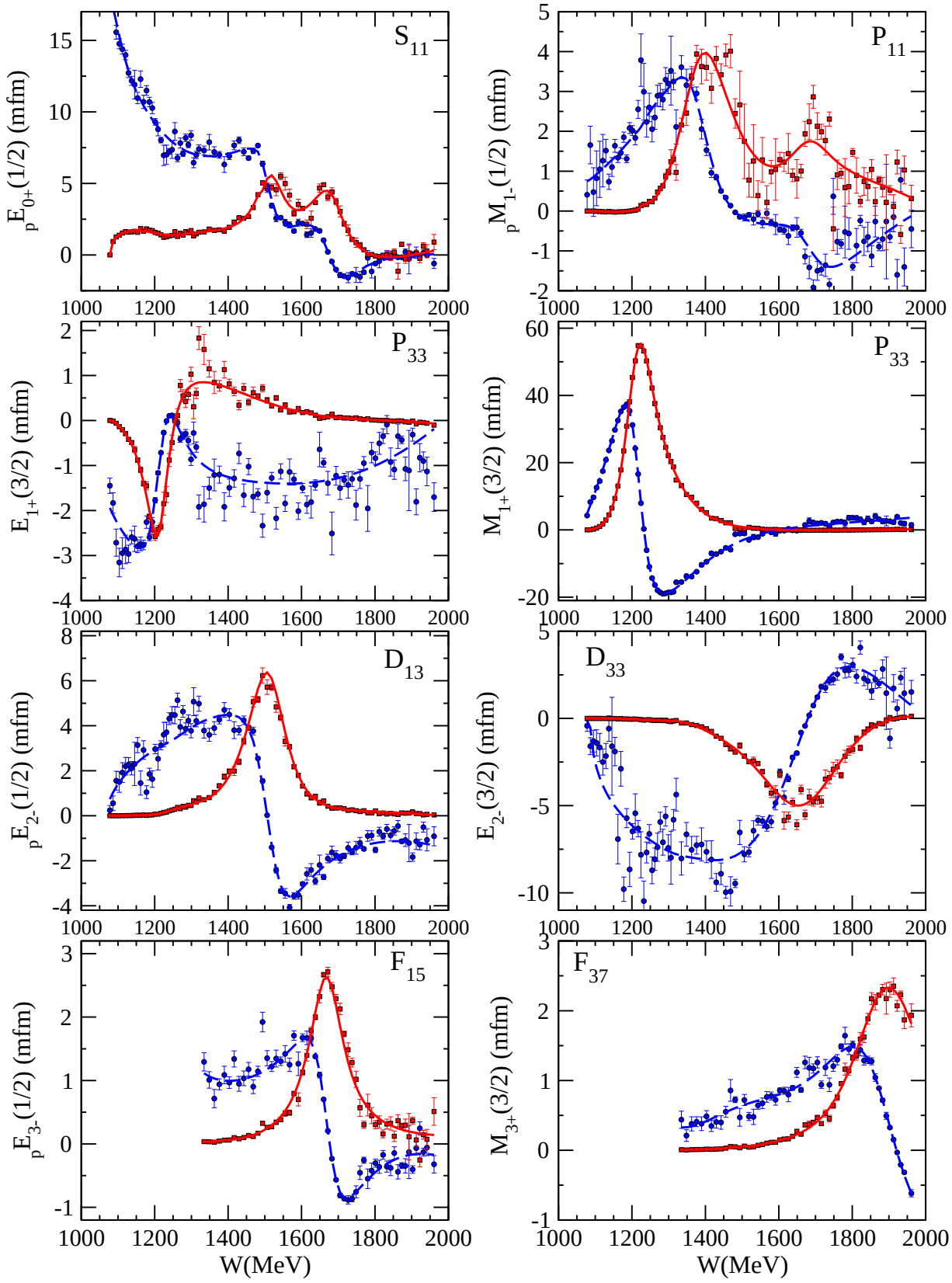

FIG. 3. L+P fit to MAID MAID2007 SE solutions. Dashed blue, and full red lines denote real and imaginary parts of multipoles respectively.

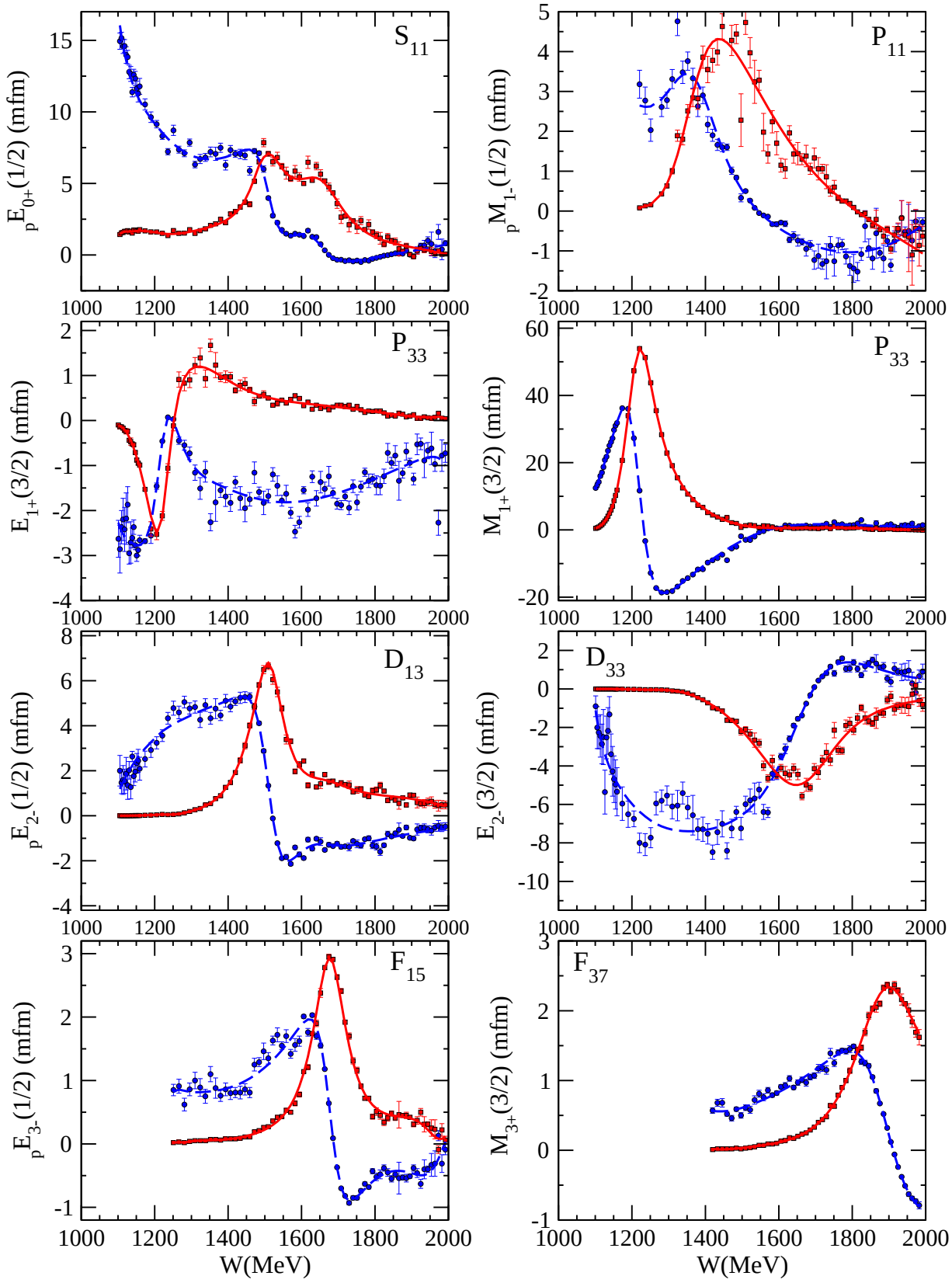

FIG. 4. L+P fit to GWU/SAID CM12 SE solutions. Dashed blue, and full red lines denote real and imaginary parts of multipoles respectively.

For the P_{33} partial wave, we have two multipoles $E_{1+}^{3/2}$ and $M_{1+}^{3/2}$. The pole of the $\Delta(1232)3/2^+$ shows up quite consistently. Only for the widths and the residues in the SE analysis we obtain 10% lower values. We also found the second state in this partial wave, the $\Delta(1600)3/2^+$ in both ED solutions with some larger deviations in the M_{1+} analysis. It is remarkable, that this resonance is found in the MAID ED solution, where it is not explicitly included in terms of a Breit-Wigner resonance, due to its status of only 3-star. However, due to the unitarization procedure in MAID, it is implicitly contained through the πN unitarization phase. For the $\Delta(1232)3/2^+$ resonance, pole positions and residues were already published in the late 90s. The numerical values which we find here with the L+P method agree very well with the pole positions and residues from $E_{1+}^{3/2}$ and $M_{1+}^{3/2}$ amplitudes in Refs. [30, 31].

The D_{13} partial wave can be analyzed in two multipoles, where the largest one, the ${}_pE_{2-}^{1/2}$ is presented here. The first state, $N(1520)3/2^-$ is very consistent in both ED and SE analyses, the second $N(1700)3/2^-$ is only found in the SAID solutions.

The D_{33} partial wave is also very important in pion photoproduction, but the photo-decay amplitudes in the Breit-Wigner parameterizations differ substantially in the PDG listings. The figures of the $E_{2-}^{3/2}$ multipoles appear very similar for MAID and SAID solutions, while the $\Delta(1700)3/2^-$ pole parameters found in our L+P expansion give a rather consistent picture. However, systematic differences between the ED and SE solutions appear much larger than the differences between MAID and SAID solutions. The newly analyzed double-polarization data of pion photoproduction will certainly tighten constraints for this state. It is worth mentioning that some structure is observed in the SE solutions of MAID and SAID around a c.m. energy of 1300 MeV, a region, where certainly no resonance is expected in this partial wave. While it looks up as a peak in the SAID solution, in MAID it appears more as a largely scattered region. Our L+P formalism cannot find any physical explanation for this structure.

The F_{15} partial wave is very similar to the previous one. In the electric ${}_pE_{3-}^{1/2}$ multipole, a very pronounced resonance structure shows up for the $N(1680)5/2^+$ state and all resonance parameters are consistently found. The second state, $N(2000)5/2^+$, another candidate for a complex ρN branch point, shows up very inconclusively in our L+P analysis. We can find it in the ED solution of MAID and in the SE solution of SAID. In the other two solutions it is not seen. The parameters clearly cannot really be considered as for the same resonance state; even the mass differs by more than 100 MeV, and the residue strength by more than an order of magnitude. The 2012 PDG tables list two states with a 2-star rating, $N(1860)5/2^+$ and $N(2000)5/2^+$. Further efforts are necessary to clarify these resonances in pion photoproduction.

The F_{37} partial wave, finally, appears rather clean both in the figures and in the resonance parameters of the $\Delta(1950)7/2^+$ state.

B. Complex branch points

In an alternative approach, we have replaced the third real branch point x_R by a complex ρN branch point, $x_R = 1708 - 70\,i$. For the P_{11}, D_{13} and F_{15} partial waves, where we already discussed problems with the second resonance states, we have found solutions that can equally well describe the partial wave data.

These results are shown in Table III. As the deviations of the fits χ^2_{dp} (D_{dp}) are almost identical in all cases, the fits to the data overlap on Figs. 1-4, so we do not show extra figures. The only way to distinguish between the two options (real vs. complex branch point) is a comparison with existing data in the three-body channel, but they have not yet been included in an analysis of the type discussed in the present study. This demonstrates quite well that either much more precise data on polarization experiments are required and/or data in different channels, as $\gamma p \to \pi\pi N$ or $\gamma p \to K\Lambda$ are badly needed in order to determine whether the resonance is formed in the two-body subsystem of a three body final state (complex Pietarinen branch point), or it is a genuine intermediate state resonance (real Pietarinen branch point).

Just as an illustration that resonance-background separation for two-body and three-body intermediate states is very different, in Fig. 5 we have compared absolute values of background and resonance contributions for the very important $P_{11}({}_pM_{1-})$ multipole.

We see that the background term contains much more structure in the complex branch point case but, lacking more data, we have to conclude that the alternative explanations are equally valid without including another channel explicitly.

TABLE III. Pole positions in MeV and residues as moduli in mfm · GeV and phases in degrees for a ρN complex branch point. The results from the L+P expansion are given for GWU/SAID and MAID energy-dependent (ED) and single-energy (SE) solutions.

Multipole	Source	Resonance	Re W_p	-2Im W_p	|residue|	θ	D_{dp}/χ^2_{dp}
$P_{11}({}_pM_{1-})$	SAID ED	$N(1440)\ 1/2^+$	1361	192	0.326	$-60°$	0.0051
	MAID ED		1367	188	0.297	$-44°$	0.0043
	MAID SE		1381	178	0.369	$-31°$	3.13
$D_{13}({}_pE_{2-})$	SAID ED	$N(1520)\ 3/2^-$	1514	109	0.371	$+16°$	0.0078
	SAID SE		1511	108	0.354	$+10°$	2.63
$F_{15}({}_pE_{3-})$	MAID ED	$N(1680)\ 5/2^+$	1662	122	0.125	$-6°$	0.0005
	SAID SE		1672	117	0.177	$-3°$	3.51

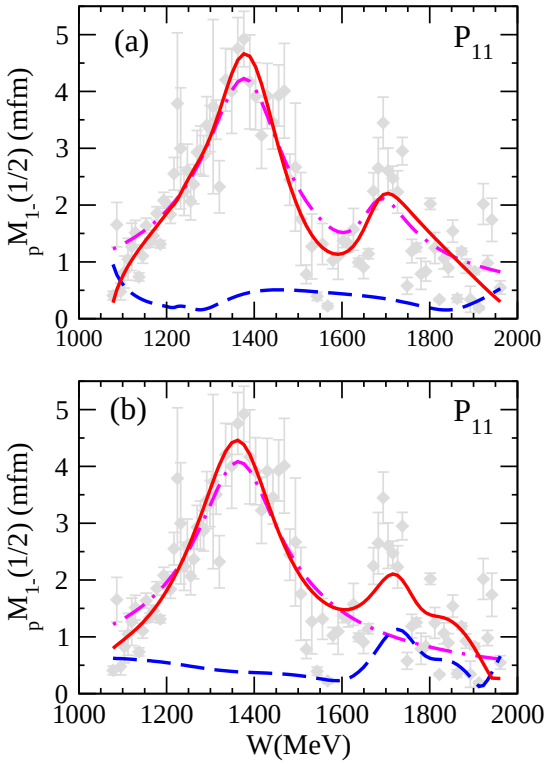

FIG. 5. Absolute values of the total amplitude, the resonance and background terms for the $P_{11}({}_pM_{1-})$ MAID SE solution are denoted by solid (red), dash-dotted (magenta) and dashed (blue) lines respectively. Figure (a) shows the result for two resonances and a real branch point, and Figure (b) shows the results for one resonance and a complex ρN branch point.

V. RESULTS AND DISCUSSION ON PHOTO-DECAY AMPLITUDES

In addition to the eight selected multipoles, which are shown in the figures and discussed above in details with respect to single energy solutions, we have also analyzed all other multipoles from the MAID and SAID ED solutions up to $L = 3$. In order to evaluate the photo-decay amplitudes of all 13 four-star resonances below $W = 2$ GeV, we also require the pole positions and residues from all other multipoles. In Table IV, we list all of these pole parameters needed for further calculations together with discrepancy parameter D_{dp} which is indicating the high quality of the fit.

Together with the results in the previous tables, we now have a complete set of e.m. residues, which allow us to relate the residues of the photoproduction multipoles to the normalized residues $(NR)^h_{\gamma,\pi}$ and to the photo-decay amplitudes A_h for helicity $h = 1/2$ and $3/2$.

For consistency with the elastic and inelastic hadronic reactions, we first introduce the unitary and dimensionless

T-matrix elements $T^h_{\gamma,\pi}$.

Following the notation of Ref. [32], the (γ,π) T-matrix element for helicity h is given by

$$T^h_{\gamma,\pi} = \sqrt{2\,k\,q}\;\mathcal{A}^h_\alpha\;C\,, \tag{6}$$

where α denotes the partial wave and k, q are the c.m. momenta of the photon and the pion. The factor C is $\sqrt{2/3}$ for isospin 3/2 and $-\sqrt{3}$ for isospin 1/2. The helicity multipoles $\mathcal{A}^h_\alpha$ are given in terms of electric and magnetic multipoles

$$\mathcal{A}^{1/2}_{\ell+} = -\frac{1}{2}\left[(\ell+2)E_{\ell+} + \ell M_{\ell+}\right], \tag{7}$$

$$\mathcal{A}^{3/2}_{\ell+} = \frac{1}{2}\sqrt{\ell(\ell+2)}\left[E_{\ell+} - M_{\ell+}\right], \tag{8}$$

$$\mathcal{A}^{1/2}_{(\ell+1)-} = -\frac{1}{2}\left[\ell E_{(\ell+1)-} - (\ell+2)M_{(\ell+1)-}\right], \tag{9}$$

$$\mathcal{A}^{3/2}_{(\ell+1)-} = -\frac{1}{2}\sqrt{\ell(\ell+2)}\left[E_{(\ell+1)-} + M_{(\ell+1)-}\right], \tag{10}$$

with $J = \ell + 1/2$ for '+' multipoles and $J = (\ell+1) - 1/2$ for '−' multipoles, all having the same total spin J.

Compared to the e.m. multipoles, which carry a dimension of length, the T-matrix elements, used here, are dimensionless and have residues defined by the pole term.

$$T^{pole,h}_{\gamma,\pi}(W) = \frac{R^h_{\gamma,\pi}}{M - W - i\Gamma/2}\,. \tag{11}$$

TABLE IV. Pole positions in MeV and residues of multipoles as moduli in mfm · GeV and phases in degrees of all multipoles needed to obtain photo-decay amplitudes.

Multipole	Source	Resonance	$\mathrm{Re}\,W_p$	$-2\mathrm{Im}\,W_p$	|residue|	θ	$10^2 D_{dp}$
$S_{31}(E_{0+})$	SAID ED	$N(1620)\,1/2^+$	$1596 \pm 3 \pm 1$	$124 \pm 6 \pm 1$	$0.332 \pm 0.019 \pm 0.002$	$(138 \pm 3 \pm 5)^\circ$	0.59
	MAID ED		$1595 \pm 2 \pm 1$	$131 \pm 3 \pm 1$	$0.423 \pm 0.009 \pm 0.003$	$(153 \pm 1 \pm 1)^\circ$	0.34
$P_{13}({}_pE_{1+})$	SAID ED	$N(1720)\,3/2^+$	$1651 \pm 7 \pm 2$	$311 \pm 15 \pm 10$	$0.108 \pm 0.001 \pm 0.008$	$-(48 \pm 3 \pm 2)^\circ$	0.07
	MAID ED		$1713 \pm 2 \pm 1$	$239 \pm 4 \pm 3$	$0.103 \pm 0.002 \pm 0.002$	$-(21 \pm 1 \pm 1)^\circ$	0.55
$P_{13}({}_pM_{1+})$	SAID ED	$N(1720)\,3/2^+$	$1637 \pm 3 \pm 14$	$307 \pm 7 \pm 10$	$0.071 \pm 0.002 \pm 0.002$	$-(148 \pm 2 \pm 20)^\circ$	0.45
	MAID ED		$1679 \pm 3 \pm 2$	$243 \pm 6 \pm 4$	$0.083 \pm 0.002 \pm 0.003$	$-(63 \pm 1 \pm 2)^\circ$	0.44
$P_{31}(M_{1-})$	SAID ED	$\Delta(1910)\,1/2^+$	$1778 \pm 16 \pm 4$	$394 \pm 35 \pm 5$	$0.356 \pm 0.037 \pm 0.016$	$-(97 \pm 5 \pm 7)^\circ$	0.07
	MAID ED		$1895 \pm 1 \pm 6$	$326 \pm 2 \pm 1$	$0.386 \pm 0.003 \pm 0.007$	$(6 \pm 1 \pm 1)^\circ$	0.93
$D_{13}({}_pM_{2-})$	SAID ED	$N(1520)\,3/2^-$	$1515 \pm 1 \pm 0$	$110 \pm 2 \pm 1$	$0.177 \pm 0.003 \pm 0.001$	$(1 \pm 1 \pm 0)^\circ$	0.41
	MAID ED		$1509 \pm 0.5 \pm 0.5$	$102 \pm 1 \pm 1$	$0.169 \pm 0.001 \pm 0.003$	$(8 \pm 0.5 \pm 0.5)^\circ$	0.46
$D_{15}({}_pE_{2+})$	SAID ED	$N(1675)\,5/2^-$	$1657 \pm 3 \pm 2$	$143 \pm 6 \pm 3$	$0.012 \pm 0.002 \pm 0.002$	$(66 \pm 3 \pm 2)^\circ$	0.33
	MAID ED		$1663 \pm 1 \pm 1$	$137 \pm 2 \pm 1$	$0.010 \pm 0.001 \pm 0.001$	$(79 \pm 1 \pm 3)^\circ$	0.25
$D_{15}({}_pM_{2+})$	SAID ED	$N(1675)\,5/2^-$	$1656 \pm 2 \pm 3$	$139 \pm 5 \pm 1$	$0.028 \pm 0.002 \pm 0.001$	$-(27 \pm 3 \pm 1)^\circ$	0.08
	MAID ED		$1658 \pm 1 \pm 6$	$138 \pm 1 \pm 1$	$0.036 \pm 0.001 \pm 0.001$	$-(20 \pm 1 \pm 0)^\circ$	0.46
$D_{33}(M_{2-})$	SAID ED	$\Delta(1700)\,3/2^-$	$1637 \pm 2 \pm 3$	$273 \pm 5 \pm 1$	$0.151 \pm 0.003 \pm 0.001$	$-(16 \pm 1 \pm 3)^\circ$	0.92
	MAID ED		$1645 \pm 1 \pm 3$	$211 \pm 2 \pm 2$	$0.125 \pm 0.001 \pm 0.002$	$-(10 \pm 1 \pm 3)^\circ$	0.93
$F_{15}({}_pM_{3-})$	SAID ED	$N(1680)\,5/2^+$	$1674 \pm 1 \pm 1$	$112 \pm 3 \pm 2$	$0.093 \pm 0.002 \pm 0.001$	$-(14 \pm 3 \pm 2)^\circ$	0.63
	MAID ED		$1642 \pm 1 \pm 10$	$123 \pm 1 \pm 1$	$0.112 \pm 0.001 \pm 0.001$	$-(11 \pm 1 \pm 0)^\circ$	0.96
$F_{35}(E_{3-})$	SAID ED	$N(1905)\,5/2^+$	$1817 \pm 5 \pm 2$	$257 \pm 12 \pm 3$	$0.049 \pm 0.003 \pm 0.001$	$(6 \pm 3 \pm 2)^\circ$	0.05
	MAID ED		$1842 \pm 4 \pm 8$	$248 \pm 8 \pm 13$	$0.017 \pm 0.002 \pm 0.002$	$-(34 \pm 2 \pm 5)^\circ$	0.09
$F_{35}(M_{3-})$	SAID ED	$N(1905)\,5/2^+$	$1815 \pm 4 \pm 2$	$266 \pm 7 \pm 1$	$0.046 \pm 0.002 \pm 0.001$	$-(20 \pm 2 \pm 2)^\circ$	0.63
	MAID ED		$1834 \pm 2 \pm 2$	$288 \pm 4 \pm 5$	$0.038 \pm 0.001 \pm 0.001$	$-(27 \pm 1 \pm 2)^\circ$	0.12
$F_{37}(E_{3+})$	SAID ED	$\Delta(1950)\,7/2^+$	$1879 \pm 3 \pm 2$	$231 \pm 7 \pm 2$	$0.014 \pm 0.001 \pm 0.001$	$-(91 \pm 2 \pm 2)^\circ$	0.98
	MAID ED		$1878 \pm 1 \pm 1$	$222 \pm 3 \pm 3$	$0.012 \pm 0.000 \pm 0.001$	$-(115 \pm 2 \pm 2)^\circ$	0.18

TABLE V. Normalized pion photoproduction T-matrix residues (dimensionless) with helicity 1/2 and 3/2 and photo-decay amplitudes in units of $GeV^{-1/2}$. The complex quantities are given in magnitudes and phases.

Resonance	source	$(NR)^{1/2}_{\gamma,\pi}$		$(NR)^{3/2}_{\gamma,\pi}$		$A_{1/2}$		$A_{3/2}$	
$\Delta(1232)\ 3/2^+$	MAID ED	0.0366(12)	128(2)°	0.0722(20)	141(2)°	0.130(2)	161(2)°	0.258(3)	174(2)°
	SAID ED	0.0363(11)	134(2)°	0.0727(18)	146(2)°	0.129(2)	167(2)°	0.259(2)	179(2)°
$N(1440)\ 1/2^+$	MAID ED	0.0165(11)	126(4)°			0.058(1)	−176(6)°		
	SAID ED	0.0156(23)	109(8)°			0.055(3)	167(11)°		
$N(1520)\ 3/2^-$	MAID ED	0.0068(7)	175(6)°	0.0480(6)	5(1)°	0.019(2)	−178(7)°	0.133(2)	12(1)°
	SAID ED	0.0100(14)	147(7)°	0.0482(25)	6(2)°	0.028(4)	154(7)°	0.133(6)	13(2)°
$N(1535)\ 1/2^-$	MAID ED	0.0276(20)	−6(10)°			0.071(3)	6(10)°		
	SAID ED	0.0289(49)	−29(9)°			0.074(10)	−17(11)°		
$\Delta(1620)\ 1/2^-$	MAID ED	0.0189(6)	−32(2)°			0.065(1)	19(2)°		
	SAID ED	0.0148(16)	−47(6)°			0.051(1)	4(9)°		
$N(1650)\ 1/2^-$	MAID ED	0.0496(38)	9(7)°			0.100(10)	46(6)°		
	SAID ED	0.0204(64)	−21(21)°			0.041(6)	16(27)°		
$N(1675)\ 5/2^-$	MAID ED	0.0038(3)	6(6)°	0.0055(3)	−40(3)°	0.016(1)	21(6)°	0.024(1)	−25(4)°
	SAID ED	0.0036(5)	10(12)°	0.0044(6)	−55(7)°	0.015(2)	25(12)°	0.019(2)	−40(8)°
$N(1680)\ 5/2^+$	MAID ED	0.0096(7)	150(5)°	0.0454(8)	−10(1)°	0.027(2)	156(5)°	0.129(2)	−4(1)°
	SAID ED	0.0049(19)	124(20)°	0.0433(17)	−12(3)°	0.014(5)	130(20)°	0.123(4)	−6(3)°
$\Delta(1700)\ 3/2^-$	MAID ED	0.0158(3)	−8(2)°	0.0166(5)	−2(3)°	0.125(2)	20(2)°	0.132(4)	27(3)°
	SAID ED	0.0141(7)	−14(2)°	0.0117(12)	−1(3)°	0.112(3)	15(3)°	0.093(7)	28(5)°
$N(1720)\ 3/2^+$	MAID ED	0.0076(3)	−41(2)°	0.0024(2)	−159(4)°	0.069(1)	17(3)°	0.022(3)	−101(2)°
	SAID ED	0.0065(6)	−72(7)°	0.0049(8)	150(9)°	0.059(2)	−14(8)°	0.045(5)	−151(11)°
$\Delta(1905)\ 5/2^+$	MAID ED	0.0019(2)	−32(5)°	0.0025(2)	144(4)°	0.017(1)	−10(6)°	0.023(1)	166(5)°
	SAID ED	0.0017(2)	−51(8)°	0.0042(2)	167(3)°	0.015(2)	−29(9)°	0.038(1)	−172(4)°
$\Delta(1910)\ 1/2^+$	MAID ED	0.0062(2)	−8(2)°			0.036(1)	−80(2)°		
	SAID ED	0.0057(7)	−111(13)°			0.033(5)	177(11)°		
$\Delta(1950)\ 7/2^+$	MAID ED	0.0182(7)	160(2)°	0.0240(9)	165(2)°	0.090(2)	−179(3)°	0.119(3)	−174(2)°
	SAID ED	0.0155(10)	154(3)°	0.0193(14)	161(3)°	0.076(4)	175(4)°	0.095(5)	−178(4)°

In Table V we list the normalized residues

$$(NR)^h_{\gamma,\pi} = \frac{R^h_{\gamma,\pi}}{\Gamma_p/2}\,, \tag{12}$$

together with the photo-decay amplitudes

$$A_h = C\sqrt{\frac{q_p}{k_p}\frac{2\pi(2J+1)W_p}{m_N Res_{\pi N}}}\,\mathrm{Res}\,\mathcal{A}^h_\alpha\,, \tag{13}$$

$$= \sqrt{\frac{\pi(2J+1)W_p}{k_p^2\, m_N Res_{\pi N}}}\; R^h_{\gamma,\pi}\,, \tag{14}$$

where the subscript p denotes quantities evaluated at the pole position. For the elastic residues, $Res_{\pi N}$, and the pole positions, $W_p = M_p - i\Gamma_p/2$, we use the values of the GWU/SAID partial wave analysis, SP06 [14].

The errors shown for the normalized residues and for the photo-decay amplitudes are obtained by error propagation from the uncertainties in the residues of the e.m. multipoles, listed in the previous tables. We considered the total errors of the E,M residues, which arise from the fitting and from the variation of the branch points. We also checked uncertainties from the pole positions, however, these errors are significantly smaller than the residue errors and can be neglected.

In almost all cases, our results in Table V show a very consistent behavior in the comparison between the analyses of the MAID and SAID solutions, with deviations mostly within $(1-2)\sigma$. An exception can be found for the $N(1650)1/2^-$. For this second resonance in the S_{11} partial wave, the normalized residues and photo-decay amplitudes

in our analyses of MAID and SAID differ by more than a factor of two. However, this is not too surprising, as a look in the Particle Data Listings show that also the Breit-Wigner amplitudes differ by more than a factor of two and even the elastic pole residues show very large deviations.

Very recently, pole values for the photo-decay amplitudes of nucleon resonances were also analyzed and published by the Bonn-Gatchina group [8], the Argonne-Osaka group [33] and the Jülich group [34]. In Tables VI and VII, we show a comparison with our current work. For many amplitudes, the magnitudes are in good agreement, while the residue phases differ quite substantially. An exception is seen in the $\Delta(1232)$ resonance, only the Jülich results are somewhat different. Similar to the elastic πN residues, where the residue phase is a measure of the non-resonant background, here also for the photoproduction residues we can assume that the residue phases give a measure of the photoproduction background contributions. And this part of the amplitude is less-well known, for most resonances, than the resonance contribution itself. In the near future the efforts in the complete experiment analysis of pseudoscalar photoproduction will certainly help to clarify this situation.

TABLE VI. Comparison of pole positions and photo-decay amplitudes in units of $GeV^{-1/2}$ between MAID (MD07), SAID (CM-12), Jülich (fit 2) [34], Bonn-Gatchina [8] and ANL-Osaka [33] for 4-star resonances with isospin 1/2.

Resonance	source	$\mathrm{Re}\,W_p$	$-2\mathrm{Im}\,W_p$	$A_{1/2}$		$A_{3/2}$	
$N(1440)\ 1/2^+$	MAID	1360(5)	183(19)	0.058(1)	$-176(6)^\circ$		
	SAID	1367(2)	190(5)	0.055(3)	$167(11)^\circ$		
	Jülich	1353	212	0.054	137°		
	BnGa	1370(4)	190(7)	0.044(7)	$142(5)^\circ$		
	ANL-O	1374	152	0.050	-12°		
$N(1520)\ 3/2^-$	MAID	1509(1)	104(8)	0.019(2)	$-178(7)^\circ$	0.133(2)	$12(1)^\circ$
	SAID	1514(2)	110(5)	0.028(4)	$154(7)^\circ$	0.133(6)	$13(2)^\circ$
	Jülich	1519	110	0.024	156°	0.117	19°
	BnGa	1507(3)	111(5)	0.021(4)	$180(5)^\circ$	0.132(9)	$2(4)^\circ$
	ANL-O	1501	78	0.038	3°	0.094	-173°
$N(1535)\ 1/2^-$	MAID	1516(3)	94(5)	0.071(3)	$6(10)^\circ$		
	SAID	1501(6)	95(11)	0.074(10)	$-17(11)^\circ$		
	Jülich	1498	74	0.050	-45°		
	BnGa	1501(4)	134(11)	0.116(10)	$7(6)^\circ$		
	ANL-O	1482	196	0.161	9°		
$N(1650)\ 1/2^-$	MAID	1678(4)	135(5)	0.100(10)	$46(6)^\circ$		
	SAID	1655(11)	127(17)	0.041(6)	$16(27)^\circ$		
	Jülich	1677	146	0.023	-29°		
	BnGa	1647(6)	103(8)	0.033(7)	$-9(15)^\circ$		
	ANL-O	1656	170	0.040	-44°		
$N(1675)\ 5/2^-$	MAID	1661(10)	138(4)	0.016(1)	$21(6)^\circ$	0.024(1)	$-25(4)^\circ$
	SAID	1657(6)	141(11)	0.015(2)	$25(12)^\circ$	0.019(2)	$-40(8)^\circ$
	Jülich	1650	126	0.022	38°	0.036	-41°
	BnGa	1654(4)	151(5)	0.024(3)	$-16(5)^\circ$	0.026(8)	$-19(6)^\circ$
	ANL-O	1650	150	0.005	-22°	0.033	-23°
$N(1680)\ 5/2^+$	MAID	1653(22)	121(6)	0.027(2)	$156(5)^\circ$	0.129(2)	$-4(1)^\circ$
	SAID	1674(3)	113(6)	0.014(5)	$130(20)^\circ$	0.123(4)	$-6(3)^\circ$
	Jülich	1666	108	0.013	120°	0.126	-24°
	BnGa	1676(6)	113(4)	0.013(4)	$155(22)^\circ$	0.134(5)	$-2(4)^\circ$
	ANL-O	1665	98	0.053	-5°	0.038	-177°
$N(1720)\ 3/2^+$	MAID	1696(22)	241(12)	0.069(1)	$17(3)^\circ$	0.022(3)	$-101(2)^\circ$
	SAID	1644(24)	309(27)	0.059(2)	$-14(8)^\circ$	0.045(5)	$-151(11)^\circ$
	Jülich	1717	208	0.051	-8°	0.014	37°
	BnGa	1660(30)	450(100)	0.110(45)	$0(40)^\circ$	0.150(35)	$65(35)^\circ$
	ANL-O	1703	140	0.234	2°	0.070	173°

TABLE VII. Same as in Table VI for 4-star resonances with isospin 3/2.

Resonance	source	$\mathrm{Re}\,W_p$	$-2\mathrm{Im}\,W_p$	$A_{1/2}$		$A_{3/2}$	
$\Delta(1232)\ 3/2^+$	MAID	1211(1)	99(1)	0.130(2)	161(2)°	0.258(3)	174(2)°
	SAID	1211(1)	101(1)	0.129(2)	167(2)°	0.259(2)	179(2)°
	Jülich	1220	86	0.114	153°	0.229	165°
	BnGa	1210(1)	99(2)	0.131(4)	161(2)°	0.254(5)	171(1)°
	ANL-O	1211	102	0.133	165°	0.257	177°
$\Delta(1620)\ 1/2^-$	MAID	1595(3)	131(4)	0.065(1)	19(2)°		
	SAID	1596(4)	124(7)	0.051(1)	4(9)°		
	Jülich	1599	71	0.028	−88°		
	BnGa	1597(4)	130(9)	0.052(5)	−9(9)°		
	ANL-O	1592	136	0.113	−1°		
$\Delta(1700)\ 3/2^-$	MAID	1647(6)	217(13)	0.125(2)	20(2)°	0.132(4)	27(3)°
	SAID	1644(12)	264(20)	0.112(3)	15(3)°	0.093(7)	28(5)°
	Jülich	1675	303	0.109	−12°	0.111	21°
	BnGa	1680(10)	305(15)	0.170(20)	50(15)°	0.170(25)	45(10)°
	ANL-O	1707	340	0.059	−70°	0.125	−75°
$\Delta(1905)\ 5/2^+$	MAID	1838(16)	268(41)	0.017(1)	−10(6)°	0.023(1)	166(5)°
	SAID	1816(8)	262(17)	0.015(2)	−29(9)°	0.038(1)	−172(4)°
	Jülich	1770	259	0.013	19°	0.072	67°
	BnGa	1805(10)	300(15)	0.025(5)	−23(15)°	0.050(4)	180(10)°
	ANL-O	1765	188	0.008	−97°	0.018	−90°
$\Delta(1910)\ 1/2^+$	MAID	1895(7)	326(3)	0.036(1)	−80(2)°		
	SAID	1778(20)	394(40)	0.033(5)	177(11)°		
	Jülich	1788	575	0.246	−133°		
	BnGa	1850(40)	350(45)	0.023(9)	40(90)°		
	ANL-O	1854	368	0.052	170°		
$\Delta(1950)\ 7/2^+$	MAID	1888(12)	247(31)	0.090(2)	−179(3)°	0.118(3)	−174(2)°
	SAID	1882(8)	231(9)	0.076(4)	175(4)°	0.095(5)	−178(4)°
	Jülich	1884	234	0.071	151°	0.089	155°
	BnGa	1890(4)	243(8)	0.072(4)	173(5)°	0.096(5)	173(5)°
	ANL-O	1872	206	0.062	171°	0.076	−178°

VI. SUMMARY AND CONCLUSIONS

In this work, we have applied the L+P method to the partial wave amplitudes of the MAID and SAID solutions for single-pion photoproduction. We have analyzed both energy-dependent and single-energy solutions, and have determined pole positions and residues from electromagnetic multipoles in the region up to $W \sim 2$ GeV. The pole positions are compared to values listed in the Particle Data Tables, and show almost perfect agreement with data coming from other channels. Presently, inelastic residues are very sparse in the Particle Data Tables, with no residues for meson photoproduction yet listed. However, since the PDG is recommending the replacement of Breit-Wigner parameters by pole parameters in future listings, we find that the L+P method, being controllably model-dependent, is a good method to extract this information from both ED and SE partial wave amplitudes.

We have found that, for all partial waves, the first resonance state can be consistently analyzed with the L+P technique and good agreement on the pole positions can be observed. This also gives us confidence in the determination of the complex residues for pion photoproduction. In the special case of the S_{11} partial wave, the second (4-star) resonance, $N(1650)1/2^-$ can be equally well analyzed, while a third $N(1895)1/2^-$ can only be found in the MAID ED solution. For most other (2- and 3-star) resonances, our analysis finds large deviations among the four different solutions. From these resonances, the $\Delta(1600)3/2^+$ is best determined, other states as $N(1710)1/2^+$, $N(1700)3/2^-$ and $N(2000)5/2^+$ give inconclusive results. All three of them, however, can alternatively be replaced by a complex branch point in the appropriate P_{11}, D_{13} and F_{15} partial waves. For these partial waves, we have demonstrated that

the amplitudes can be similarly described by either a real branch point and two resonances or a complex branch point and only one resonance.

Furthermore, for all partial waves, we have investigated the four-star resonances in the energy region $W < 2$ GeV with respect to the normalized T-matrix residues and the photo-decay amplitudes at the pole positions. We have compared our results with other very recently published analyses and find good agreement for dominant amplitudes, but also considerable deviations for smaller amplitudes or amplitudes of nucleon resonances that are less well determined.

In conclusion, we have found that a single-channel partial wave analysis can consistently determine the pole position and parameters of the lowest nucleon resonances, but cannot distinguish between higher resonances and alternative complex branch points. However, with the additional information of other decay channels, especially with three-body final states, a unique determination should be possible.

ACKNOWLEDGMENTS

This work was supported in part by the U.S. Department of Energy Grant DE-FG02-99ER41110, the Deutsche Forschungsgemeinschaft (SFB 1044).

APPENDIX

Tables VIII and IX compare results with the third branch point either fixed, based on the threshold for a dominant inelastic channel, or allowed to adjust for a best fit. The variation is used in the estimation of systematic errors, as discussed in Section III.B.

TABLE VIII. Parameters from L+P expansion are given for GWU/SAID and MAID energy dependent (ED) solutions. N_r is the number of resonance poles, x_P, x_Q, x_R are branch points in MeV.

Multipole	Source									
	SAID ED					MAID ED				
	N_r	x_P	x_Q	x_R	$10^2 D_{dp}$	N_r	x_P	x_Q	x_R	$10^2 D_{dp}$
$S_{11}({}_pE_{0+})$	2	142	$1077^{\pi N}$	$1215^{\pi\pi N}$	0.49	3	-3778	$1077^{\pi N}$	$1215^{\pi\pi N}$	1.20
	2	900	$1077^{\pi N}$	$1486^{\eta N}$	0.35	3	-131	$1077^{\pi N}$	$1486^{\eta N}$	1.01
	2	889	$1077^{\pi N}$	1495^{free}	0.31	3	-393	$1077^{\pi N}$	1379^{free}	0.98
$P_{11}({}_pM_{1-})$	2	900	$1077^{\pi N}$	$1215^{\pi\pi N}$	0.13	2	309	$1077^{\pi N}$	$1215^{\pi\pi N}$	0.31
	2	900	$1077^{\pi N}$	$1370^{Real(\pi\Delta)}$	0.15	2	494	$1077^{\pi N}$	$1370^{Real(\pi\Delta)}$	0.28
	2	871	$1077^{\pi N}$	1375^{free}	0.12	2	123	$1077^{\pi N}$	1515^{free}	0.15
$P_{33}({}_pE_{1+})$	2	883	$1077^{\pi N}$	$1215^{\pi\pi N}$	0.12	2	838	$1077^{\pi N}$	$1215^{\pi\pi N}$	0.20
	2	899	$1077^{\pi N}$	$1370^{Real(\pi\Delta)}$	0.12	2	167	$1077^{\pi N}$	$1370^{Real(\pi\Delta)}$	0.19
	2	818	$1077^{\pi N}$	1218^{free}	0.09	2	534	$1077^{\pi N}$	1222^{free}	0.09
$P_{33}(M_{1+})$	2	900	$1077^{\pi N}$	$1215^{\pi\pi N}$	0.08	2	-5238	$1077^{\pi N}$	$1215^{\pi\pi N}$	1.29
	2	788	$1077^{\pi N}$	$1370^{Real(\pi\Delta)}$	0.05	2	-218	$1077^{\pi N}$	$1370^{Real(\pi\Delta)}$	1.50
	2	507	$1077^{\pi N}$	1238^{free}	0.02	2	900	$1077^{\pi N}$	1265^{free}	0.89
$D_{13}({}_pE_{2-})$	2	900	$1077^{\pi N}$	$1215^{\pi\pi N}$	0.28	1	485	$1077^{\pi N}$	$1215^{\pi\pi N}$	0.35
	2	832	$1077^{\pi N}$	$1370^{Real(\pi\Delta)}$	0.34	1	528	$1077^{\pi N}$	$1370^{Real(\pi\Delta)}$	0.33
	2	900	$1077^{\pi N}$	$1700^{Real(\rho N)}$	0.36	1	48	$1077^{\pi N}$	$1700^{Real(\rho N)}$	0.17
	2	900	$1077^{\pi N}$	1232^{free}	0.28	1	898	$1077^{\pi N}$	1717^{free}	0.06
$D_{33}({}_pE_{2-})$	1	900	$1077^{\pi N}$	$1215^{\pi\pi N}$	0.18	1	900	$1077^{\pi N}$	$1215^{\pi\pi N}$	0.45
	1	537	$1077^{\pi N}$	$1370^{Real(\pi\Delta)}$	0.19	1	609	$1077^{\pi N}$	$1370^{Real(\pi\Delta)}$	0.46
	1	900	$1077^{\pi N}$	1105^{free}	0.15	1	900	$1077^{\pi N}$	1222^{free}	0.34
$F_{15}({}_pE_{3-})$	1	900	$1077^{\pi N}$	$1215^{\pi\pi N}$	0.01	2	899	$1077^{\pi N}$	$1215^{\pi\pi N}$	0.11
	1	856	$1077^{\pi N}$	$1370^{Real(\pi\Delta)}$	0.02	2	883	$1077^{\pi N}$	$1370^{Real(\pi\Delta)}$	0.14
	1	898	$1077^{\pi N}$	$1700^{Real(\rho N)}$	0.02	2	898	$1077^{\pi N}$	$1700^{Real(\rho N)}$	0.12
	1	900	$1077^{\pi N}$	1222^{free}	0.01	2	-118	$1077^{\pi N}$	1126^{free}	0.10
$F_{37}({}_pE_{3+})$	1	897	$1077^{\pi N}$	$1370^{Real(\pi\Delta)}$	0.01	1	-1931	$1077^{\pi N}$	$1370^{Real(\pi\Delta)}$	0.03
	1	755	$1077^{\pi N}$	$1700^{Real(\rho N)}$	0.01	1	-977	$1077^{\pi N}$	$1700^{Real(\rho N)}$	0.03
	1	900	$1077^{\pi N}$	1285^{free}	0.01	1	-215	$1077^{\pi N}$	1230^{free}	0.02

TABLE IX. Parameters from L+P expansion are given for GWU/SAID and MAID single energy (SE) solutions. N_r is the number of resonance poles, x_P, x_Q, x_R are branch points in MeV.

Multipole	Source									
	MAID SE					SAID SE				
	N_r	x_P	x_Q	x_R	χ^2_{dp}	N_r	x_P	x_Q	x_R	χ^2_{dp}
$S_{11}({}_pE_{0+})$	2	-950	$1077^{\pi N}$	$1215^{\pi\pi N}$	3.88	2	-9935	$1077^{\pi N}$	$1215^{\pi\pi N}$	3.02
	2	-395	$1077^{\pi N}$	$1486^{\eta N}$	3.86	2	-4986	$1077^{\pi N}$	$1486^{\eta N}$	2.53
	2	876	$1077^{\pi N}$	1491^{free}	3.53	2	556	$1077^{\pi N}$	1499^{free}	2.47
$P_{11}({}_pM_{1-})$	2	-1037	$1077^{\pi N}$	$1215^{\pi\pi N}$	3.03	1	-1256	$1077^{\pi N}$	$1215^{\pi\pi N}$	3.02
	2	-810	$1077^{\pi N}$	$1370^{Real(\pi\Delta)}$	2.74	1	-12191	$1077^{\pi N}$	$1370^{Real(\pi\Delta)}$	3.05
	2	-3417	$1077^{\pi N}$	1362^{free}	2.73	1	-10673	$1077^{\pi N}$	1324^{free}	2.97
$P_{33}({}_pE_{1+})$	1	-2754	$1077^{\pi N}$	$1215^{\pi\pi N}$	3.38	1	754	$1077^{\pi N}$	$1215^{\pi\pi N}$	3.00
	1	-1759	$1077^{\pi N}$	$1370^{Real(\pi\Delta)}$	3.34	1	615	$1077^{\pi N}$	$1370^{Real(\pi\Delta)}$	3.02
	1	46	$1077^{\pi N}$	1467^{free}	3.21	1	-1267	$1077^{\pi N}$	1155^{free}	2.98
$P_{33}(M_{1+})$	1	-1670	$1077^{\pi N}$	$1215^{\pi\pi N}$	3.26	2	-1116	$1077^{\pi N}$	$1215^{\pi\pi N}$	2.94
	1	-7265	$1077^{\pi N}$	$1370^{Real(\pi\Delta)}$	3.27	2	60	$1077^{\pi N}$	$1370^{Real(\pi\Delta)}$	2.86
	1	-387	$1077^{\pi N}$	1250^{free}	3.24	2	639	$1077^{\pi N}$	1236^{free}	2.84
$D_{13}({}_pE_{2-})$	1	-6892	$1077^{\pi N}$	$1215^{\pi\pi N}$	2.77	2	775	$1077^{\pi N}$	$1215^{\pi\pi N}$	2.68
	1	-96	$1077^{\pi N}$	$1370^{Real(\pi\Delta)}$	2.79	2	716	$1077^{\pi N}$	$1370^{Real(\pi\Delta)}$	2.66
	1	-232	$1077^{\pi N}$	$1700^{Real(\rho N)}$	3.02	2	831	$1077^{\pi N}$	$1700^{Real(\rho N)}$	2.57
	1	900	$1077^{\pi N}$	1193^{free}	2.61	2	179	$1077^{\pi N}$	1737^{free}	2.33
$D_{33}({}_pE_{2-})$	1	862	$1077^{\pi N}$	$1215^{\pi\pi N}$	5.04	1	638	$1077^{\pi N}$	$1215^{\pi\pi N}$	2.53
	1	835	$1077^{\pi N}$	$1370^{Real(\pi\Delta)}$	4.71	1	837	$1077^{\pi N}$	$1370^{Real(\pi\Delta)}$	2.45
	1	899	$1077^{\pi N}$	1556^{free}	4.61	1	-663	$1077^{\pi N}$	1374^{free}	2.36
$F_{15}({}_pE_{3-})$	1	-27038	$1077^{\pi N}$	$1215^{\pi\pi N}$	3.63	2	900	$1077^{\pi N}$	$1215^{\pi\pi N}$	3.34
	1	-923	$1077^{\pi N}$	$1370^{Real(\pi\Delta)}$	3.93	2	-139	$1077^{\pi N}$	$1370^{Real(\pi\Delta)}$	3.26
	1	-715	$1077^{\pi N}$	$1700^{Real(\rho N)}$	3.08	2	900	$1077^{\pi N}$	$1700^{Real(\rho N)}$	2.86
	1	90	$1077^{\pi N}$	1705^{free}	3.03	2	-165	$1077^{\pi N}$	1717^{free}	2.69
$F_{37}({}_pE_{3+})$	1	894	$1077^{\pi N}$	$1370^{Real(\pi\Delta)}$	2.49	1	-146	$1077^{\pi N}$	$1370^{Real(\pi\Delta)}$	1.66
	1	70	$1077^{\pi N}$	$1700^{Real(\rho N)}$	2.06	1	667	$1077^{\pi N}$	$1700^{Real(\rho N)}$	1.68
	1	-247	$1077^{\pi N}$	1649^{free}	1.87	1	-1504	$1077^{\pi N}$	1270^{free}	1.64

[1] J. Beringer et al. (Particle Data Group), Phys. Rev. **D86**, 010001 (2012).
[2] International Workshop on New partial wave analysis tools for next generation hadron spectroscopy experiments, June 20-22, 2012, Camogli, Italy. [http://www.ge.infn.it/∼athos12].
[3] ATHOS 2013-International Workshop on New Partial-Wave Analysis Tools for Next-Generation Hadron Spectroscopy Experiments, 21-24 May 2013 Kloster Seeon, Germany, [http://intern.universe-cluster.de/indico/event/2857].
[4] M. Döring, C. Hanhart, F. Huang, S. Krewald, and U.-G. Meißner, Nucl. Phys. **A829**, 170 (2009), and references therein.
[5] B. Juliá-Díaz, H. Kamano, T.-S. H. Lee, A. Matsuyama, T. Sato, N. Suzuki, Phys. Rev. **C80**, 025207 (2009), and references therein.
[6] R. E. Cutkosky, C. P. Forsyth, R. E. Hendrick, and R. L. Kelly, Phys. Rev. **D 20**, 2839 (1979).
[7] M. Batinić, I. Šlaus, A. Švarc, and B. M. K. Nefkens, Phys. Rev. **C 51**, 2310 (1995); M. Batinić et al., Phys. Scr. **58**, 15 (1998).
[8] A. V. Anisovich, R. Beck, E. Klempt, V. A. Nikonov, A. V. Sarantsev, U. Thoma, Eur. Phys. J. **A48**, 15 (2012); [http://pwa.hiskp.uni-bonn.de/], and references therein.
[9] G. Höhler, πN Newsletter **9**, 1 (1993).
[10] N.G. Kelkar, M. Nowakowski, Phys. Rev. **A78**, 012709 (2008), and references therein.
[11] G. F. Chew and S. Mandelstam, Phys. Rev. **119**, 467 (1960).
[12] S. Ceci, J. Stahov, A. Švarc, S. Watson, and B. Zauner, Phys. Rev. **D 77**, 116007 (2008).
[13] A. Švarc, M. Hadžimehmedović, H. Osmanović, J. Stahov, L. Tiator, R. L. Workman, Phys. Rev. **C 88**, 035206 (2013).
[14] R. A. Arndt, W. J. Briscoe, I. I. Strakovsky, and R. L. Workman, Phys. Rev. **C 74**, 045205 (2006); [http://gwdac.phys.gwu.edu/analysis/]
[15] R. L. Workman, R. A. Arndt, W. J. Briscoe, M. W. Paris, and I. I. Strakovsky, Phys. Rev. **C 86**, 035202 (2012).
[16] G. Y. Chen, S. S. Kamalov, S. N. Yang, D. Drechsel, and L. Tiator, Phys. Rev. **C 76**, 035206 (2007).
[17] L. Tiator, S. S. Kamalov, S. Ceci, Guan Yeu Chen, D. Drechsel, A. Svarc, and Shin Nan Yang, Phys. Rev. **C 82**, 055203 (2010).
[18] R. L. Workman, M. W. Paris, W. J. Briscoe, L. Tiator, S. Schumann, M. Ostrick, S. S. Kamalov, Eur. Phys. J. **A47**, 143 (2011).
[19] A. V. Anisovich, R. Beck, E. Klempt, V. A. Nikonov, A. V. Sarantsev, U. Thoma and Y. Wunderlich, Eur. Phys. J. A **49**, 121 (2013).
[20] M. Hazewinkel: *Encyclopaedia of Mathematics*, Vol. 6, Springer, 1990, p. 251.
[21] S. Ciulli and J. Fischer, Nucl. Phys. 24, 465 (1961).
[22] I. Ciulli, S. Ciulli, and J. Fischer, Nuovo Cimento **23**, 1129 (1962).
[23] E. Pietarinen, Nuovo Cimento **12A**, 522 (1972).
[24] G. Höhler, *Pion Nucleon Scattering*, Part 2, Landolt-Börnstein: Elastic and Charge Exchange Scattering of Elementary Particles, Vol. 9b (Springer-Verlag, Berlin, 1983).
[25] C. G. Boyd, B. Grinstein, and R. F. Lebed, Phys. Rev. Lett. **74**, 4603 (1995); R. J. Hill, and G. Paz, Phys. Rev. **D 82**, 113005 (2010).
[26] V.N. Gribov, 'Strong Interactions of hadrons at high energies', Cambridge U. Press, 2009.
[27] S. Ceci, M. Döring, C. Hanhart, S. Krewald, U.-G. Meißner, and A. Švarc, Phys. Rev. **C 84**, 015205 (2011).
[28] D. Drechsel, S. S. Kamalov and L. Tiator, Eur. Phys. J. A **34**, 69 (2007);[http://www.kph.uni-mainz.de/MAID/].
[29] A. Švarc, M. Hadžimehmedović, R. Omerović, H. Osmanović, J. Stahov, arXiv:1401.1947 [nucl-th].
[30] O. Hanstein, D. Drechsel and L. Tiator, Phys. Lett. B **385**, 45 (1996).
[31] R. L. Workman and R. A. Arndt, Phys. Rev. C **59**, 1810 (1999).
[32] R. L. Workman, L. Tiator and A. Sarantsev, Phys. Rev. C **87**, 068201 (2013).
[33] H. Kamano, S. X. Nakamura, T. -S. H. Lee and T. Sato, Phys. Rev. C **88**, 035209 (2013).
[34] D. Rönchen, M. Döring, F. Huang, H. Haberzettl, J. Haidenbauer, C. Hanhart, S. Krewald and U. -G. Meißner *et al.*, arXiv:1401.0634 [nucl-th].